Eliminating material dependency in spectra measurement via non-neighbouring band regression

Hui-Liang Shen,[a],* Quan-Geng Ge,[a] Zhi-Huan Zheng,[a] Xin Du,[a] Si-Jie Shao[b] and John H. Xin[b]

[a]*College of Information Science and Electronic Engineering, Zhejiang University, Hangzhou 310027, China*
Email: shenhl@zju.edu.cn

[b]*Institute of Textiles and Clothing, The Hong Kong Polytechnic University, Hong Kong, China*

A multispectral imaging system, after necessary calibration, can measure the spectral reflectances of colour samples accurately at a high spatial resolution. A limitation is that agreement of its measurements with those of a reference spectrophotometer is affected by the reflective characteristics of sample materials. The state-of-the-art methods aim to improve interinstrument agreement using the spectral values of neighbouring bands. However, it is observed that non-neighbouring bands are more effective in modelling interinstrument agreement. Inspired by this observation, the present paper proposes a method for eliminating material dependency by least-squares regression among non-neighbouring spectral bands. The fundamental issue of band selection is solved using a binary differential evolution algorithm. Experimental results confirm that the proposed method is effective in reflectance correction in terms of both spectral and colorimetric accuracy. The method is of practical application to multispectral imaging systems when measuring the spectral reflectances of colour samples with different materials.

Introduction

Nowadays, multispectral imaging is attracting intense interest owing to its unique ability to measure colour spectra at a high spatial resolution. Its operating principle is to divide the visible spectrum into more than three bands and transform camera response to spectral reflectance.

Figure 1 illustrates a typical multispectral imaging system that consists of a monochrome camera and a filter wheel installed with a set of filters. The lighting direction is 45° with respect to the sample surface normal, and the viewing direction coincides with the surface normal. This is in accordance with the CIE recommended 45°/normal geometry. The multispectral imaging system is calibrated using calibration samples such that its reflectance measurement agrees with a reference spectrophotometer. As we know, a high-precision spectrophotometer usually adopts the diffuse/8° geometry, in which the diffuse illumination is produced by an integrating sphere. Owing to the different geometries, the interinstrument agreement will be affected by the reflective characteristics (e.g. gloss) of the samples. Figure 2 illustrates two slices of bidirectional reflectance distribution functions (BRDFs) [1] of two materials, *A* and *B*, at a given lighting direction. These two materials have only diffuse reflection, but the reflective characteristics are obviously different. Because of this, if the multispectral imaging system is calibrated using samples with material *A*, its measurement agreement with the spectrophotometer will degrade when measuring samples with material *B*.

The problem of material influence in colour imaging has been noted in previous work [2,3]. Although it is possible to eliminate material dependency [4] by adjusting the calibration transform, in this work we simply regard the multispectral imaging system as a colour measurement instrument without knowing its calibration details. With this treatment, material dependency elimination is similar to interinstrument agreement improvement [5–8].

In the literature, several methods have been proposed to improve the interinstrument agreement. For example, Berns and Petersen [5] derived a generic model that has seven terms. These terms include the offset, band value, first- and second-order derivatives of band value, quadratic band value, and two non-linearly scaled derivatives of band value. Rich and Martin [6] simplified this generic model to avoid possible overfitting by using four terms, i.e. the offset, band value, and its first- and second-order derivatives. Reniff [7] also modified the Berns and Petersen model [5] by incorporating high-order reflectance factors. Chung *et al.* [8] introduced the R-model with four terms, which are the offset, band value, and forward and backward neighbouring band values. It has been shown [9], that with a proper mathematical manipulation, the R-model is equivalent to the Rich and Martin model [6]. A recent comprehensive review indicates that the three-band R-model is the most reliable method to date [9]. It is worth noting that all the mentioned methods improve the interinstrument agreement based on fixed neighbouring bands.

In this paper, we observe from experiment that the non-neighbouring bands are more effective in eliminating material dependency, or equivalently, improving interinstrument agreement (see the ground truth correction matrices in Figure. 5). This indicates that the neighbouring band constraint employed in the state-of-the-art methods is too restrictive and actually not necessary. Motivated by this, we propose a novel method for modelling material dependency by applying least-squares regression on non-neighbouring bands. The fundamental issue of band selection is effi-
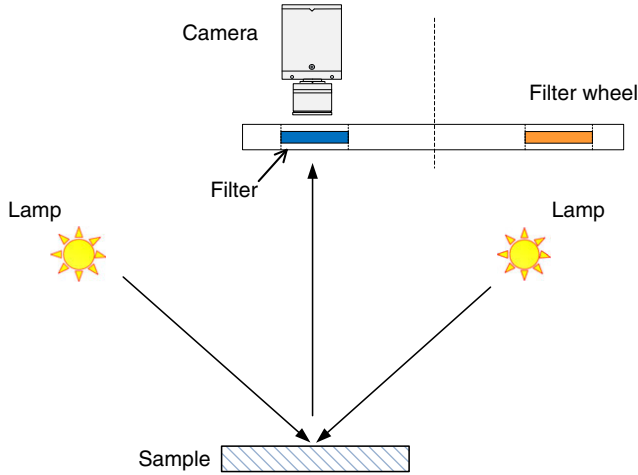
Figure 1 Schematic diagram of a typical multispectral imaging system [Colour figure can be viewed in the online issue, which is available at wileyonlinelibrary.com.]

ciently solved by using a novel binary differential evolution algorithm. The reliability of the proposed method is evaluated using two different materials, i.e. textile Pantone samples and printed paper samples. To our knowledge, this is the first work that aims to eliminate material dependency, or improve interinstrument agreement, by using non-neighbouring spectral bands.

Background

In the following, we briefly review the principle of multi-spectral imaging and reflectance reconstruction. Assume the visible spectrum, whose wavelength range is usually from 400 to 700 nm in practical computation, is divided into N samples, and the multispectral imaging system contains C channels. In this work, $N = 31$ and $C = 16$. According to the imaging model, the camera response $\mathbf{u} \in R^C$ of a sample with spectral reflectance $\mathbf{r} \in R^N$ is formulated as

$$\mathbf{u} = \mathbf{Mr} + \mathbf{n} \tag{1}$$

where $\mathbf{n}$ denotes imaging noise. The matrix $\mathbf{M}$ is the spectral responsivity of the system, which combines the spectral power distribution of the illuminant, the spectral transmittance of the filter, and the spectral sensitivity of the camera. A fundamental issue in multispectral imaging is to compute the spectral reflectance $\mathbf{s}$ from the camera response $\mathbf{u}$ via a calibration transform $\mathbf{W}$ such that

$$\mathbf{s} = \mathbf{Wu} \tag{2}$$

is a close replica of $\mathbf{r}$. The matrix $\mathbf{W}$ can be computed using various techniques such as least squares, finite-dimension modelling [10], or Wiener estimation [10,11]. In the calibration process, the spectral reflectance $\mathbf{r}$ is measured using a reference spectrophotometer.

To eliminate material dependency, our objective is to find a correction matrix $\mathbf{A}$ that maps the reflectance $\mathbf{s}$ measured by the multispectral imaging system to the reflectance $\mathbf{r}$ measured by the spectrophotometer. Mathematically, the correction process is formulated as

$$\mathbf{r} = \mathbf{A}\tilde{\mathbf{s}} \tag{3}$$

where $\tilde{\mathbf{s}} = (\mathbf{s}^T, 1)^T$ is an augmented version of $\mathbf{s}$, and consequently $\mathbf{A}$ is of dimension $N \times (N+1)$, with its last column referred to as the offset vector.

In the R-model [8], the correction of band value $r(n)$ is conducted on three neighbouring bands:

$$r(n) = a_{n-1}s(n-1) + a_n s(n) + a_{n+1}s(n+1) + a_0 \tag{4}$$

Suppose L training samples are available in the correction process, the coefficients a_{n-1}, a_n, a_{n+1}, and a_0 can be computed using least squares. By writing the coefficients of all N bands together, the correction matrix of the R-model becomes

$$\mathbf{A}_{R-model} = \begin{pmatrix} a_{11} & a_{12} & 0 & 0 & \dots & 0 & 0 & 0 & a_{10} \\ a_{21} & a_{22} & a_{23} & 0 & \dots & 0 & 0 & 0 & a_{20} \\ 0 & a_{32} & a_{33} & a_{34} & \dots & 0 & 0 & 0 & a_{30} \\ & \dots & & & \dots & & & \dots & \\ 0 & 0 & 0 & 0 & \dots & 0 & a_{N,N-1} & a_{N,N} & a_{N0} \end{pmatrix} \tag{5}$$

As observed, it has non-zero elements only in neighbouring bands.

From the perspective of linear regression, the essence of the R-model [8] and the relevant methods [5–7] is to model the relationship between a scalar dependent variable $r(n)$ with several explanatory variables that are empirically fixed in neighbouring bands. The problem is that, although these predetermined explanatory variables produce low regression error, they are still not the optimal ones in explaining the dependent variable. In this regard, we aim to find the explanatory variables that have better explanation capability by breaking the neighbouring band limitation.
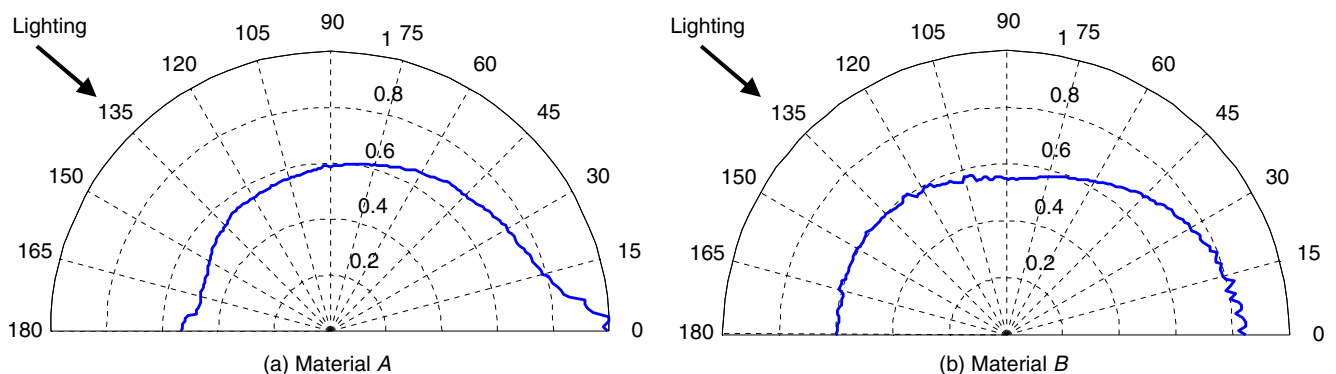

Figure 2 BRDF slices of two materials (*A* and *B*) in the incident plane [Colour figure can be viewed in the online issue, which is available at wileyonlinelibrary.com.]

Proposed method

The proposed non-neighbouring band regression method will be elaborated as follows. In the following, we first consider the modelling of the specific nth band ($1 \leq n \leq N$). To apply the binary differential evolution algorithm, we define a binary row vector $\mathbf{x} \in R^N$ for the nth band as

$$\mathbf{x} = (\, 0 \quad 1 \quad 0 \quad 0 \quad 1 \quad \ldots \quad 0 \quad 1 \quad 0 \,) \qquad (6)$$

In vector $\mathbf{x}$, a bit value 1 indicates that the corresponding band is selected, and otherwise unselected. If K bands are involved in computation, $\mathbf{x}$ will contain K bits with value 1.

In addition to the selected bands specified by vector $\mathbf{x}$, we also use an offset in the proposed method. Let $\tilde{\mathbf{x}} = (\mathbf{x}, 1)$ be the augmented version of $\mathbf{x}$, and $\mathbf{a}_n$ be the nth row vector of matrix $\mathbf{A}$ specified in Eqn (3), then the row vector

$$\tilde{\mathbf{a}}_n(\mathbf{x}) = \mathbf{a}_n \text{diag}(\tilde{\mathbf{x}}) \qquad (7)$$

contains the $K + 1$ non-zero elements of $\mathbf{a}_n$. Here diag($\cdot$) transforms a vector to its diagonal matrix counterpart.

To correct the nth band of the reflectance, the objective function is defined as the total regression error on L training samples:

$$f_n(\mathbf{x}) = \sum_{i=1}^{L} (\, \tilde{\mathbf{a}}_n(\mathbf{x}) \bar{\mathbf{s}}_i - r_i(n))^2 \qquad (8)$$

where $r_i(n)$ is the value of band n and $\bar{\mathbf{s}}_i \in R^{K+1}$ are the selected band values of the augmented reflectance defined in Eqn (3). To find the optimal bands, we need to find the vector $\mathbf{x}$ that minimises the objective function given in Eqn (8).

In the binary differential evolution algorithm, let N_P be the number of individuals in the population, and G be the maximum number of generations, then $\mathbf{x}_{g,i}$ denotes the ith individual in the gth generation. For our problem, the number of bits with values 1 in vector $\mathbf{x}$ should be kept as K in the evolution procedure. We define the difference between two randomly selected candidate vectors, $\mathbf{x}_{g,i}$ and $\mathbf{x}_{g,j}$, as a table of swapping pairs with bit values 0 and 1:

$$T_{ij} = \mathbf{x}_{g,i} \otimes \mathbf{x}_{g,j} \qquad (9)$$

where the binary-cross operator $\otimes$ produces the indices of swapping pairs in T_{ij}. For example, $T_{ij} = \begin{pmatrix} 1 & 7 & 13 \\ 3 & 10 & 14 \end{pmatrix}$ means that (1,3), (7,10), and (13,14) are three swapping pairs.

In the mutation operation, a trial vector $\mathbf{v}_{g,k}$ is generated as

$$\mathbf{v}_{g,k} = \mathbf{x}_{g,k} \oplus T_{ij} \qquad (10)$$

where the binary-plus operator $\oplus$ swaps the bit values of the indices of $\mathbf{x}_{g,k}$ according to the swapping pairs specified in table T_{ij}.

In the selection operation, the trial vector $\mathbf{v}_{g,k}$ competes with the current solution $\mathbf{x}_{g,k}$ according to the objective function (8), and the solution vector passing to the next generation is determined as

$$\mathbf{x}_{g+1,k} = \begin{cases} \mathbf{v}_{g,k} & \text{if } f_n(\mathbf{v}_{g,k}) < f_n(\mathbf{x}_{g,k}) \\ \mathbf{x}_{g,k} & \text{otherwise.} \end{cases} \qquad (11)$$

The binary differential evolution algorithm repeats the above mutation and selection operations in each generation, and the final optimal solution is determined as

$$\mathbf{x}_{\text{opt}} = \text{argmin} \, f_n(\mathbf{x}_{G,k}), k \in \{1, 2, \ldots, N_P\} \qquad (12)$$

Note that the $\mathbf{x}_{\text{opt}}$ is optimal for the nth band. By applying the binary differential evolution algorithm on all N bands, we can obtain the correction matrix $\mathbf{A}$ whose non-zero elements are determined by N optimal solution vectors.

In the binary differential evolution algorithm, we set the number of individuals $N_P = \left[\begin{pmatrix} N \\ K \end{pmatrix}^{1/3} \right]$, where N and K are the numbers of total and selected bands, and the operator $[\cdot]$ rounds the variable to its nearest integer. The initial individuals are randomly generated. Our investigation indicates that the algorithm always converges in fewer than 20 generations, irrespective of population initialisation. Figure 3 illustrates the distribution of spectral root mean square (rms) error with respect to the number of generations for a certain population initialisation. The convergence distributions for other population initialisations are similar. Based on this observation, we set the maximum number of generations $G = 20$.
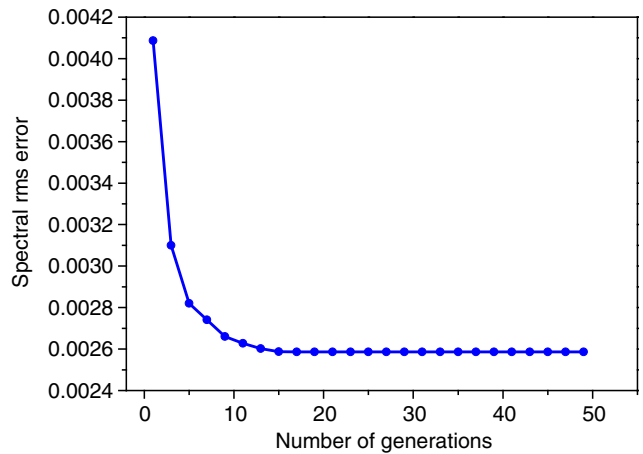

Figure 3 Distribution of spectral rms errors with respect to the number of generations of the binary differential evolution algorithm [Colour figure can be viewed in the online issue, which is available at wileyonlinelibrary.com.]
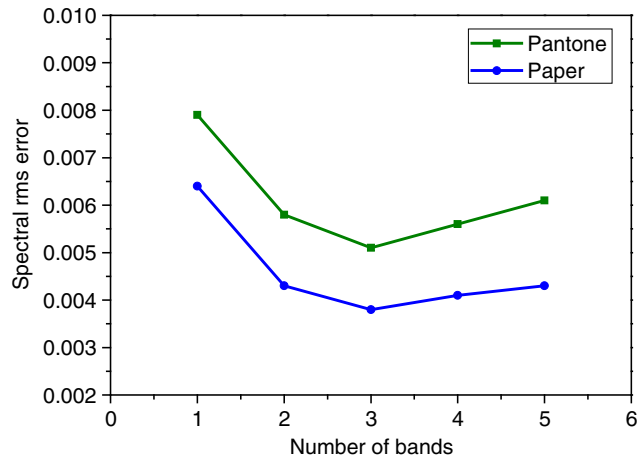

Figure 4 Distributions of spectral rms errors with respect to the number of spectral bands for the proposed method [Colour figure can be viewed in the online issue, which is available at wileyonlinelibrary.com.]
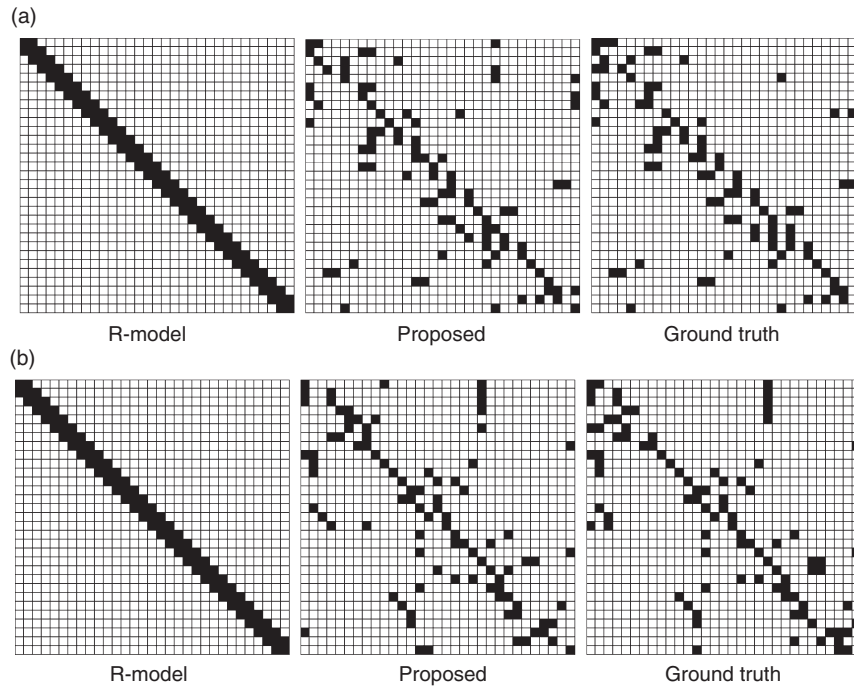
(a)

R-model　　　　　　Proposed　　　　　　Ground truth

(b)

R-model　　　　　　Proposed　　　　　　Ground truth

Figure 5 The $N \times N$ submatrices of the correction matrices **A**, excluding the offset vector, for (a) Pantone and (b) paper materials. The non-zero elements are filled in black
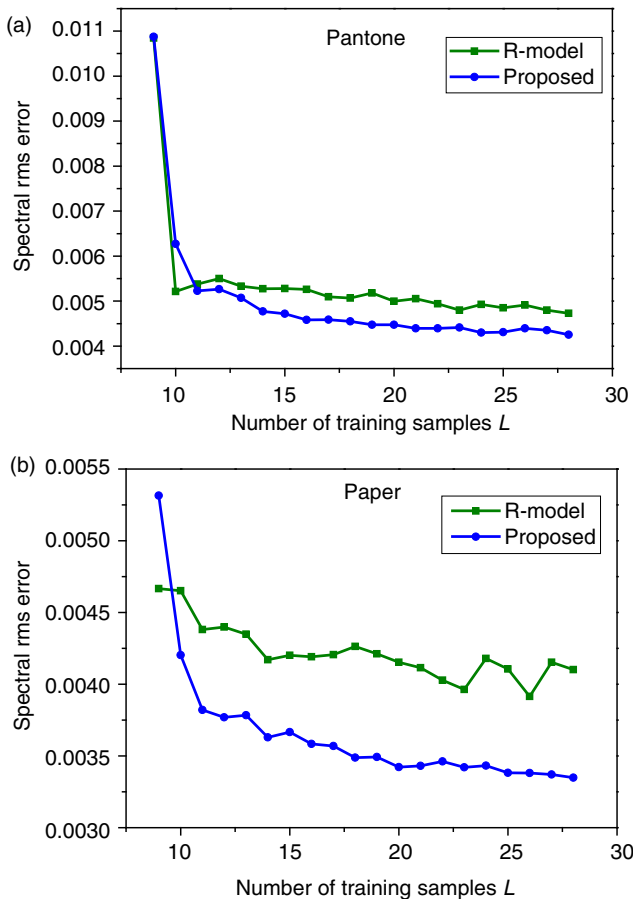
(a)

(b)

Figure 6 Distributions of spectral rms errors with respect to the number of training samples [Colour figure can be viewed in the online issue, which is available at wileyonlinelibrary.com.]

Experiments

The multispectral imaging system includes a 14-bit scientific monochrome camera and a filter wheel installed with 16 narrow band filters. A set of tungsten lamps were employed to

Table 1 Spectral rms errors of the R-model and proposed method. Lowest errors are in bold

Material	Method	Spectral rms		
		Mean	Median	Max
Pantone	w/o correction	0.0236	0.0230	0.0597
	R-model	0.0055	0.0049	0.0173
	Proposed	**0.0051**	**0.0044**	**0.0169**
Paper	w/o correction	0.0256	0.0244	0.0539
	R-model	0.0044	0.0041	00109
	Proposed	**0.0038**	**0.0037**	**0.0093**

illuminate the samples uniformly at the 45° direction. In terms of CIEDE2000 colour difference ΔE_{00} [12], the current colorimetric accuracy of the multispectral imaging system is around 0.3 units, and the repeatability accuracy is 0.05 units. We consider the system approximately meets the requirement of a colour measurement instrument.

Three sets of samples with different materials were used, including (a) 96 colours on the X-Rite Digital ColorChecker SG (X-Rite, Inc., USA), which are referred to as SG samples hereafter, (b) 144 randomly selected textile Pantone samples, and (c) 108 paper samples printed using a six-ink EPSON colour printer (Stylus Photo 1390; Epson, Japan). The spectral reflectance data of all these samples were measured using a reference Datacolor SF600 spectrophotometer (Datacolor, USA). The SG samples were employed to calibrate the multispectral imaging system, and the Pantone and paper samples were employed to test the proposed method. The colour accuracy was evaluated using CIEDE2000 colour difference under typical CIE illuminants (A, D65, and F2), as well as spectral rms error defined as

$$e = \frac{1}{\sqrt{N}}||\mathbf{r} - \mathbf{A}\tilde{\mathbf{s}}||_2 \tag{13}$$

where N is the number of bands.

Table 2 Colorimetric errors of the R-model and proposed method in terms of CIEDE2000 colour difference under illuminants D65, A, and F2. Lowest errors are in bold

Material	Method	ΔE_{00} under D65			ΔE_{00} under A			ΔE_{00} under F2		
		Mean	Median	Max	Mean	Median	Max	Mean	Median	Max
Pantone	w/o correction	2.14	1.89	5.06	2.08	1.84	5.15	2.14	1.90	5.15
	R-model	0.55	0.43	2.67	0.51	0.41	2.21	0.57	0.43	2.67
	Proposed	**0.45**	**0.38**	**2.34**	**0.45**	**0.38**	**1.91**	**0.42**	**0.37**	**1.47**
Paper	w/o correction	3.04	2.88	6.48	2.89	2.71	6.70	3.16	2.97	6.54
	R-model	0.46	0.40	2.85	0.45	0.39	2.75	0.45	**0.35**	2.02
	Proposed	**0.38**	**0.34**	**1.14**	**0.37**	**0.34**	**1.09**	**0.40**	0.35	**1.30**
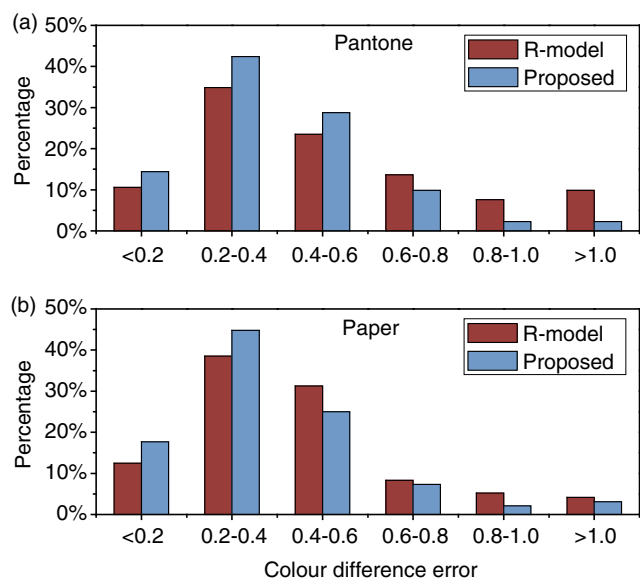
Figure 7 Distributions of colour difference errors of the R-model and the proposed method [Colour figure can be viewed in the online issue, which is available at wileyonlinelibrary.com.]

The samples in sets (b) and (c) were individually divided into a subset of training samples and a subset of test samples. The training samples were sequentially determined by maximising the condition number, i.e. the ratio between the maximum and minimum eigenvalues, of the matrix of selected reflectances [13]. In this way, the training samples should be representative of the whole sample set.

It is necessary to determine the appropriate number of bands, K, in the non-neighbouring band regression using the training samples. Theoretically, the value of K can vary for individual bands. Our investigation reveals that using varying K values produces a minor improvement in spectral accuracy but does not yield better colorimetric accuracy. This is because of the non-linear relationship between the spectral and colorimetric metrics. Therefore, we used the same value of K for all bands in the proposed method.

Figure 4 shows the distributions of spectral rms errors with respect to the number of spectral bands in the case of using $L = 12$ training samples. For both Pantone and paper materials, we obtain the lowest spectral errors when $K = 3$. The use of more bands will degrade the spectral accuracy owing to overfitting.

Figure 5 illustrates the patterns of selected bands of the $N \times N$ submatrix of the correction matrix **A**, excluding the offset vector. There are $K = 3$ selected bands in each row of the submatrix. The ground truths are obtained from the training and test samples by exhaustive search of the bands. More clearly, in total $\binom{31}{3}$, combinations of three bands were evaluated. For each combination, the correction matrix **A** was computed from the training samples, and the average spectral rms error of the test samples was computed using this matrix. The band combination that produces the minimum spectral rms error was regarded as the ground truth. It can be seen from Figure 5 that the ground truth bands were sparsely distributed, which is opposite to the basic assumption of the R-model. Owing to the binary differential evolution algorithm, the proposed method can efficiently compute the correction matrix, which is quite close to the ground truth, from the training samples.

It is of interest to investigate whether the number of training samples has an influence on the proposed method. Figure 6 shows that, for both Pantone and paper materials, the spectral rms errors decrease when more training samples are used. It can be seen that the distributions are quite different for the Pantone and paper materials. Figure 6 shows that, when the number of training samples L is larger than 12, the proposed method performs better than the R-model. In the following, we show quantitative results when using $L = 12$ training samples. This is a reasonable choice to use a minimum number of training samples in practical applications, provided that the required colour accuracy is satisfied. We note that the distributions of spectral rms errors can be different when evaluated on samples with different sizes, but we will not show the details in this paper.

Table 1 shows the spectral rms errors of the R-model and proposed method for the test samples. As indicated, without reflectance correction, the mean spectral rms errors are very large (0.023) for both materials. The mean spectral rms errors produced by the proposed method are 0.0051 and 0.0038 for the Pantone and paper materials respectively. Despite the seemingly slight improvement over the R-model, the statistical Wilcoxon signed rank test [14] confirms that the resultant spectral rms errors of the proposed method are lower than those of the R-model at a significance level $p = 0.01$.

Table 2 shows that the resultant mean colour difference error of the proposed method is around 0.45 units for the Pantone samples and is below 0.40 units for the paper
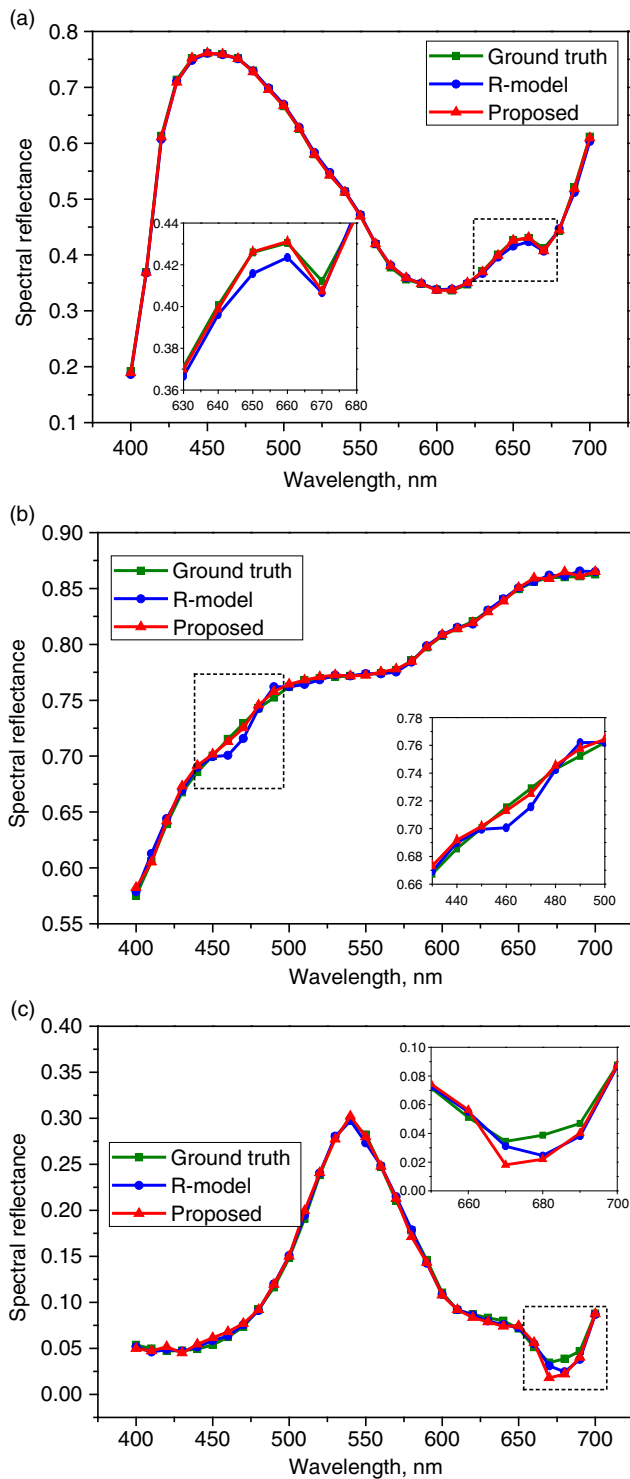
Figure 9 The worst case of spectral reflectance correction by the proposed method [Colour figure can be viewed in the online issue, which is available at wileyonlinelibrary.com.]

errors for the Pantone and paper materials under illuminant D65. These two distributions further verify that the colour difference errors produced by the proposed method are lower than those of the R-model.

Figure 8 shows the corrected spectral reflectance curves of three samples for illustration purposes. For the colour samples in (a) and (b), the reflectance curves produced by the proposed method are closer to the actual ones when compared with the R-model. For the colour sample in (c), the version corrected by the R-model is more satisfactory. This observation is consistent with the quantitative results shown in Tables 1 and 2. The proposed method performs statistically better than the R-model, but can still produce less satisfactory results on certain samples.

Figure 9 shows the worst case produced by the proposed method, which corresponds to a Pantone colour sample. The spectral rms error of this sample is 0.0169 and the CIEDE2000 colour difference error is 2.34 units under illuminant D65. This indicates that the correction matrix computed from the training samples cannot well explain the material dependency of this sample. Nevertheless, the proposed method still produces slightly better reflectance correction when compared with the R-model.

Conclusions

In this paper, we have proposed a method for eliminating material dependency in a multispectral imaging system via non-neighbouring band regression. By employing the binary differential evolution algorithm, the proposed method is able to find the optimal reflectance bands and outperforms the existing method in terms of both spectral and colorimetric accuracy. As the proposed method does not involve detailed calibration of the multispectral imaging system, it can also be employed to improve the interinstrument agreement between spectrophotometers.

Acknowledgements

Figure 8 Three examples of spectral reflectance correction by the R-model and the proposed method. The insets show the parts highlighted in boxes with dot borders [Colour figure can be viewed in the online issue, which is available at wileyonlinelibrary.com.]

samples. The maximum errors of the Pantone material are 2.34 and 1.91 units under the D65 and A illuminants respectively. These large values are produced by a dark sample whose spectral rms error is actually quite low. This is because of the non-linear relationship between the spectral error and the colorimetric error. The statistical test shows that the proposed method outperforms the R-model in terms of colorimetric error metric at a significance level $p = 0.01$. Figure 7 shows histograms of the CIEDE2000
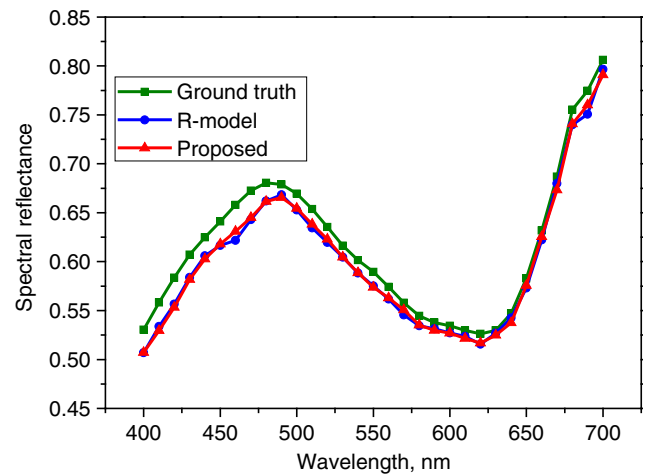
References

1. F E Nicodemus, J C Richmond, J J Hsia, I W Ginsberg and T Limperis, *Radiometry* (Sudbury: Jones and Bartlett Publishers, 1992).
2. G Hong, M R Luo and P A Rhodes, *Color Res. Applic.*, **26** (2001) 76.
3. Y Murakami, T Obi, M Yamaguchi, N Ohyama and Y Komiya, *Opt. Commun.*, **188** (2001) 47.
4. H L Shen, C W Weng, H J Wan and J H Xin, *J. Opt. Soc. Am. A*, **28** (2011) 511.
5. R S Berns and K H Pertersen, *Color Res. Applic.*, **13** (1988) 243.
6. D C Rich and D Martin, *Analyt. Chim. Acta*, **380** (1999) 263.
7. L Reniff, *Color Res. Applic.*, **19** (1994) 332.
8. Y S Chung, J H Xin and K M Sin, *Color. Technol.*, **120** (2004) 284.
9. Y Xu, M R Luo, P L Sun and C Li, *Color. Technol.*, **129** (2013) 312.
10. H L Shen, J H Xin and S J Shao, *Opt. Express*, **15** (2007) 5531.
11. W K Pratt, *Digital Image Processing*, 4th Edn (New York: Wiley, 2007).
12. M R Luo, G Cui and B Rigg, *Color Res. Applic.*, **26** (2011) 340.
13. J Y Hardeberg, *Acquisition and Reproduction of Color Images: Colorimetric and Multispectral Approaches* (Paris: Ecole Nationale Superieure des Telecommunications, 1999).
14. R V Hogg and E A Tanis, *Probability and Statistical Inference* (Englewood Cliffs, NJ: Prentice Hall, 2001).